

Ozone Loss Inside the Northern Polar Vortex During the 1991-1992 Winter

M. H. Proffitt, K. Aikin, J. J. Margitan, M. Loewenstein, J. R. Podolske, A. Weaver,
K. R. Chan, H. Fast and J. W. Elkins

M. H. Proffitt and K. Aikin are with the NOAA Aeronomy lab, 325 Broadway, Boulder, Colorado 80303 and CIRES, University of Colorado, Boulder, Colorado 80309. J. J. Margitan is with the Jet Propulsion Laboratory, California Institute of Technology, Pasadena, CA 91109. M. Loewenstein, J. R. Podolske, A. Weaver, and K. R. Chan are with the NASA Ames Research Center, Moffett Field, CA 94035. H. Fast is with Atmospheric Environmental Service, Downsview, Ontario M3H 51'4, Canada. J. W. Elkins is with NOAA CMDL, 325 Broadway, Boulder, Colorado 80303.

June 16, 1993

ABSTRACT

Measurements made in the outer ring of the northern polar vortex from October 1991 through March 1992 reveal an altitude dependent change in ozone, with decrease at the bottom of the vortex and substantial increase at the highest altitudes accessible. The increase is the result of ozone rich air entering the vortex, and the decrease reflects ozone loss accumulated after descent through high concentrations of reactive chlorine. The depleted air that is released out of the bottom of the vortex is sufficient to significantly reduce column ozone at mid-latitudes.

During the Antarctic late winter and early spring, the decrease in ozone (O_3) due to anthropogenic chemical loss is sufficient to overwhelm the naturally occurring increase due to transport of O_3 rich air from lower latitudes (1). The dearth of O_3 is obvious in column measurements and has been called an O_3 hole. The seasonal onset of the chemical O_3 loss is not as easily observed since it is masked by increases due to transport (2, 3). In the Northern Hemisphere vortex, the period of significant loss is relatively short, due to the warmer less stable Arctic vortex dissipating by late winter. In this case, a weaker loss is overwhelmed by a stronger seasonal increase due to transport (4, 5). Although an O_3 hole does not form, the Arctic vortex contains less O_3 than normal.

Concern over O_3 loss recently intensified with reports of significant column O_3 decrease over the heavily populated mid-latitudes in all seasons and both hemispheres (6). These mid-latitude changes are not completely understood (7), but

it appears that the decreases are due to chemistry occurring at mid-latitudes (8) and transport of O_3 poor air from polar to mid-latitudes (2, 4, 9, 10).

In 1991-1992 the second NASA-NOAA Airborne Arctic Stratospheric Expedition (AASE II) was undertaken to investigate the cause of the mid-latitude O_3 decreases and to assess the possibility of an ozone hole occurring in the Northern Hemisphere during this century. Daytime measurements of atmospheric chemical and dynamical components were made simultaneously at high latitudes from October through March. Three flights out of Fairbanks, Alaska (65° N) from 6-12 October flew to or near the pole, followed by 17 flights out of Bangor, Maine (45° N), from 12 December through 20 March, of which 8 penetrated the polar vortex.

In this report we use AASE II measurements from instruments (11) aboard the NASA ER-2 high altitude aircraft to evaluate offsetting effects of chemical O_3 destruction and transport by analyzing the evolution of chemical species in the outer ring of the winter vortex (12). We focus on the vertical distribution of change in O_3 , the causes of the observed change, and whether loss of O_3 in the polar vortex can account for the winter mid-latitude O_3 decrease.

O_3 is naturally produced and destroyed through photochemistry that occurs in the stratosphere. Before about 1980, the minimum of sunlight that occurs during polar winter was insufficient to trigger substantial O_3 production or destruction (13), but with our present elevated concentrations of stratospheric chlorine, rapid O_3 loss can occur.

To distinguish change in O_3 (mixing ratio by volume) due to transport from loss due to chemistry, we adopt a method using an empirically derived functional relation between a conserved tracer, nitrous oxide (N_2O) (14), and O_3 (4, 15, 16). The function is used as a reference for O_3 and represents simultaneous measurements of O_3 and N_2O before wintertime loss has occurred. Because N_2O has a lifetime of years, changes from the reference reflect recent changes in O_3 . The difference between a measured value of O_3 and a reference value calculated from the simultaneously measured N_2O represents the wintertime loss (17).

Daily meteorological and chemical data show that the vortex perimeter wobbled considerably during AASE II, so identifying its location along each flight leg is critical to our analysis of the vortex interior. The boundary of the polar vortex has been previously defined in a variety of ways, including (i) the region of very high chlorine monoxide (ClO) (18) (ii) the peak in the wind speed (4) (iii) threshold values in potential vorticity (PV) (10, 19) or its maximum gradient (20) and (iv) gradients in N_2O and water vapor (21). Elevated concentrations of reactive chlorine were usually found in the polar vortex (22) and indicated significant O_3 destruction was underway. Concentrations of the reactive chlorine species ClO were very high on every flight that penetrated the polar jet from December through March (23), so we defined the vortex boundary to exclude all data with $ClO < 150$ pptv from the vortex interior and to exclude data clearly outside the dynamical boundary (Table 1). Our boundaries are conservative in the sense that some parcels experiencing loss (high ClO) lie slightly outside the boundary, and no air from outside the dynamical vortex is included within the boundary.

For a vertical coordinate, we used potential temperature (a measure of

entropy and denoted by Θ), which increases with altitude and is calculated from measured temperature and pressure (24). In the absence of wave induced mixing and diabatic cooling, air parcels will stay on constant Θ (isentropic) surfaces. Although altitude is more intuitive as a vertical coordinate, it is less useful at high latitudes during the winter months, particularly when an understanding of transport is required. In our coordinate system, diabatic cooling is equivalent to descent. We define $\Theta = 410 \pm 10$ K as the bottom of the vortex (4), suggesting relatively free exchange of air with lower latitudes at and below that level (25).

O_3 increased inside the vortex from October through March by about 1000 ppbv (part per billion by volume) at all values of Θ (Fig. 1A). However, the steady (isentropic temporal) increase was interrupted by a small decrease in O_3 of about 250 ppbv from December into January below 460 K. From late January through March the O_3 mixing ratios were nearly constant below 460 K, but continued to increase above that level. These increases are due to O_3 rich air that has been transported to high latitudes. The result is a 50% increase in the column O_3 between 15 and 20 km from October through mid February.

Over the same period and above 460 K, O_3 also increased substantially relative to N_2O , but O_3 significantly decreased below that level (Fig. 1B). These changes in O_3 for a constant N_2O are evident comparing the raw data of October with February data (Fig. 2A). The greatest O_3 decrease was found below the bottom of the vortex during the months of January and February (Fig. 2B).

A quadratic fit (26) to the October O_3 - N_2O data is given by

$$O_3^{OCT}(\text{ppbv}) = 1682 + 18.62X N_2O(\text{ppbv}) - 0.0798X (N_2O(\text{ppbv}))^2 \quad (1)$$

with $N_2O > 130$ ppbv and $\sigma = 172$ ppbv

and we use this function as the October reference (27). We denote measured mixing ratios of O_3 by O_3^M , thus, change in O_3 since the October reference period can be simply viewed as statistical change in the quantity $O_3^M - O_3^{OCT}$. There are three types of air parcels we distinguish by comparison with the October reference:

(i) type I: $O_3^M - O_3^{OCT} > 2\sigma$ (increased O_3)

(ii) type D: $O_3^M - O_3^{OCT} < -2\sigma$ (decreased O_3)

(iii) type 0: $-2\sigma \leq (O_3^M - O_3^{OCT}) \leq 2\sigma$ (unchanged O_3).

Whether a parcel is of type I, 0, or D depends upon its O_3 content relative to N_2O in October (the parcel's initial O_3 - N_2O relation) and the photochemical production and loss of O_3 in that parcel since October.

Parcels of type I have increased O_3 that must be attributed to photochemical production or to an initial O_3 - N_2O relation that differs from the October data, i.e. air that was not sampled in October. O_3 production is not responsible for the increase observed, because average production rates during the winter are apparently much less than the measured rate of increase (28). However, if during October, parcels of type I are above ER-2 altitudes, then descent (decreasing Θ) in

the vortex during the following months might contribute to the increase. N_2O generally decreases with increasing θ , and $N_2O > 130$ ppbv would not be expected to persist above ER-2 altitudes. As N_2O decreases, O_3 is expected to increase at these θ 's. Simultaneous measurements of N_2O and O_3 at higher θ 's have never been made at high latitudes in October, so no direct verification is available. In lieu of these measurements, we used sonde data for October 1991 at five θ levels from 530 K to 610 K for each of two high latitude stations, Resolute (75° N) and Alert (82° N) verifying the increase of O_3 with increasing θ . This sonde data along with ER-2 data allowed us to extend the O_3^{OCT} reference to N_2O mixing ratios of 50 ppbv and $\theta = 610$ K (29) (Fig. 2C). This extended reference implies that neither descent in the vortex, nor mixing of higher altitude air ($N_2O < 130$ ppbv) with air of type O can produce the increased O_3 in parcels of type I found in later months. An influx of air from outside the vortex is apparently the only source available for the increase.

To verify this we have compared the $O_3 - N_2O$ relation for pi reels of type I with a linear fit to the December through March data from outside the vortex (30). The fit is given by

$$O_3^{EXT} \text{ (ppbv)} = 7172 - 23.06X N_2O \text{ (ppbv)} \quad (2)$$

with $N_2O > 150$ ppbv and $\sigma = 240$ ppbv

and agrees very well with the $O_3 - N_2O$ relation for parcels of type I (Fig. 2C). This suggests that the increase in O_3 is due to air that penetrated the vortex.

A confirmation of this result is provided by the January and February $O_3 - N_2O$ data. If the interior of the vortex were isolated from its exterior at some θ level, two disjoint $O_3 - N_2O$ relations would develop as O_3 increased outside the vortex due to transport, and was chemically destroyed preferentially inside. However, we found that for θ 's accessible to the ER-2, the $O_3 - N_2O$ relations were practically indistinguishable over their common range of N_2O (Fig. 2D). At the bottom of the vortex, with $\theta < 420$ K, air parcels are of type D, both inside and outside the boundary and appear as a single line. This is consistent with relatively free exchange of O_3 poor air latitudinally at and below the bottom of the vortex. At the highest flight levels, with $\theta > 500$ K, the parcels are practically all of type I. Although the two data sets still have identical overlap, they appear as two nearly intersecting lines. This is not consistent with free exchange across the boundary, but does indicate that lower latitude parcels have penetrated the vortex. Apparently, parcels with N_2O of about 150 ppbv have recently entered at this level and still have their exterior character, while other parcels have apparently mixed with vortex air of lower N_2O content. This has produced the line of vortex data characteristic of mixing (Fig. 2D). Although not shown in our figures, all isentropic levels above the bottom of the vortex were similar to the $\theta > 500$ K level, showing distinct somewhat linear data sets with common overlap. This indicates that air penetrated the vortex at all flight altitudes.

We found virtually no air parcels with $N_2O < 140$ ppbv outside the vortex boundary (31), indicating that air deep inside the vortex with $N_2O \ll 140$ ppbv did not escape the vortex and retain its identity in the process. This does not exclude

vortex peel-off (10) as a contributor of vortex edge material at mid-latitudes..

Parcels of type D contain less O_3 which must be attributed to photochemical loss or to an initial $O_3 - N_2O$ relation below the O_3^{OCT} reference. Diabatic cooling (descent) rather than diabatic heating dominated throughout the period, and descent inside the vortex without O_3 loss will increase rather than decrease O_3 relative to N_2O (Fig. 1B). Air outside the vortex is rich in O_3 and cannot directly account for the decrease. We conclude that the dominant cause of the decrease in O_3 must be photochemical loss that has occurred during winter.

Why was O_3 constant at 460 K? Diabatic cooling was taking place, so air with enhanced O_3 must have descended through the 460 K isentrope. This should have increased O_3 relative to N_2O , so lack of change represents a close balance between the increase "due to transport (including descent) and photochemical loss. Transport similarly masks O_3 loss at all levels throughout the outer vortex.

To quantify the offsetting effects of transport and photochemical loss, we calculated average daily loss rates, flight-by-flight, from December through March for air parcels of types I, O, and D (Table 2). We assumed conservatively only 6 hours of daily solar exposure and restricted N_2O to mixing ratios common to all three parcel types (Fig. 2C). A relatively weak O_3 loss began by mid-December (Fig. 3A). In early January, the rate of O_3 destruction% increased substantially and was greatest in parcels of type L. By mid-January, the destruction rate was greatest for parcels of type O and D, although the mixing ratios of ClO were comparable (32) (see Table 2). By mid-February, the O_3 destruction in type I parcels had decreased significantly, but remained relatively high for types O and D. This is because i) air parcels initially of type I lost O_3 and became parcel types O and D, and ii) relatively unprocessed air of type I (i.e. containing lower levels of reactive chlorine) had been transported into the vortex, and hence had a lower O_3 destruction rate.

Comparison of the calculated O_3 loss rates with the measured rates of O_3 change (Table 2) show the measured rates underestimate loss in all parcel types (Fig. 3A, B). Transport induced increases even dominated the significant loss rates calculated at the highest levels.

Although much is understood about high latitude O_3 photochemistry, our understanding of polar vortex dynamics is far from complete and the topic is somewhat controversial. The dispute began for the Antarctic and extended to the Arctic, concentrating on whether the vortex is an isolated air mass (33) or not (2, 4, 21, 34). Advocates of isolation argue that both polar vortices define a region of highly isolated air (35), and that polar loss has virtually no effect on mid-latitude O_3 before the vortex breaks up. They also argue there is one-way transport from the vortex edge to mid-latitudes as the vortex erodes. The opposing view contends the vortex is a flowing processor, with O_3 rich air entering and depleted or processed air (i.e. air high in reactive chlorine) leaving the vortex region. Supporters of the flowing processor claim that replenishment of vortex O_3 descending flow through the vortex, and peeling off of processed edge material must be accounted for to accurately evaluate the mass of O_3 destroyed due to polar processes and its subsequent dilution of O_3 at lower latitudes (2). The flowing processor has been

criticized with dynamical arguments claiming that poleward fluxes into the vortex are not significant (35, 36).

The O_3 change over the winter months can be conservatively estimated inside and outside the vortex at various θ 's directly from the O_3^{OCT} reference (Fig. 4A). This reference ignores poleward transport as required for an isolated vortex. If instead, we assume there was sufficient poleward flow of air into the outer ring of the vortex to replace the October air with exterior air, then O_3 loss accumulated over the period would be better estimated using O_3^{EXT} (Fig. 4B). This approach is considered as an upper limit for the loss accumulated, particularly for December when parcels remaining from October might still be descending through the vortex. The O_3^{OCT} analysis indicates only small isentropic gradients in O_3 change when crossing into the vortex, while the O_3^{EXT} analysis reveals the abrupt increase in loss expected in the region of highly elevated reactive chlorine. Although no loss was found above 460 K using O_3^{OCT} , the loss calculated with O_3^{EXT} (Fig. 4B) compares well with the 25% at 18 km obtained from AASE II lidar measurements (25) and with the 20% at $\theta = 470$ K calculated with a photochemical model that utilized AASE 11 measurements and meteorological tracer data (37). However, the larger decrease we found at lower θ 's (using both references) and the mixture of depleted and enhanced O_3 we found at and below the bottom of the vortex outside its boundary (Fig. 4B), has not been reported by others. The altitude distribution of O_3 decrease outside is consistent with the altitude distribution of the long term decrease reported from sonde and from satellite measurements (38). Fig. 4B portrays a vortex that is not an impenetrable container, nor is it unconstrained with no sides and no bottom. For each θ level outside the boundary, the vortex can be pictured as a leaky bucket: fluid enters the bucket over the lip (air enters the vortex at a θ level), the walls of the bucket restrict the fluid as it descends and mixes with fluid already in the bucket (air descends and mixes inside the vortex), until it exits through the leaky bottom (until it reaches the vortex bottom where it is released).

We define the O_3 mass deficit, ϑ , of a portion of the atmosphere as the mass of O_3 lost relative to a reference O_3 content, and is calculated as

$$\vartheta = k \int [w \times A \times (O_3^M - O_3^{REF}) \times \rho] dt \quad (3)$$

where ρ is the air density, O_3^{REF} is either O_3^{OCT} or O_3^{EXT} , w is the rate of parcel descent at the bottom of the vortex, A is the area of descent, and k is a constant (mass/ O_3 molecule). We calculated vertical velocities from -70 meters/day in early winter to -55 meters/day in late winter, and the outer ring of the vortex was assumed as the area of descent (39). When O_3 loss is thus integrated from 12 December, 1991 through 20 March, 1992, we obtained $\vartheta = 9$ megatons (MT) for the case using the October reference and $\vartheta = 18$ MT using the exterior reference (Fig. 3C). These deficits correspond to 1.3 % and 2.6 % respectively of the total mass of O_3 from 30° to 60° N (700 MT), a significant part of the 4% average wintertime mid-latitude column O_3 decrease observed over the past decade (6). Descending air that is deeper inside the vortex, air that is spun-off from the side of the vortex, and the release of depleted air at the time of the vortex demise will also contribute to the O_3 mass lost at high latitudes.

Table 1. Vortex boundaries and Θ 's at boundary for flights in the data in analysis (40). Boundaries are such that $\text{ClO} > 150$ pptv at all latitudes poleward of its location (except during dives) and it was coincident or poleward of steep meridional gradients in N_2O and PV.

Flight date	Flight Leg	Lat & Θ at Boundary		Maximum Lat ("N)
		(ON)	(K)	
6 Oct., 1991		pre-vortex		85
8 Oct., 1991		pre-vortex		90
12 Oct., 1991		pre-vortex		90
12 Dec., 1991	Northbound	64	480	68
	Southbound	64	490	
4 Jan., 1992	Northbound	59	460	65
	Southbound	57	475	
16 Jan., 1992	Northbound	62	470	69
	Southbound	62	480	
20 Jan., 1992	Northbound	51	460	68
	Southbound	48	495	
13 Feb., 1992	Northbound	57	480	69
	Southbound	55	505	
17 Feb., 1992	Northbound	55	470	69
	Southbound	54	505	
20 Mar., 1992	Northbound	62	500	67
	Southbound	56	520	

Table 2. Averages of ten second Θ , O_3 , N_2O and ClO data for parcels of type I, O and D (Fig. 2c). All data are inside the vortex and $130 \text{ ppbv} < N_2O < 180 \text{ ppbv}$. $O_3@155$ is the average O_3 normalized to $N_2O = 155 \text{ ppbv}$ by using the measured value for dO_3/dN_2O . O_3 loss rates (dO_3/dt) are calculated from averaged ten second measurements of $[ClO]^2$ and by assuming six hours of daily solar exposure and altitude dependent bromine monoxide concentrations that are consistent with 1989 AASE data (41). The loss rates represent the forward rate of ClO dimer formation along with the reactions of ClO with BrO. Temperature dependent rate constants are from the 1992 JPL compilation (42).

Flight date	Θ (K)	O_3 (ppbv)	$O_3@155$ (ppbv)	N_2O (ppbv)	ClO (pptv)	dO_3/dt (ppbv/day)
12 Dec., 1991						
I	477	3035	2982	153	340	-3.42
O	464	2774	2774	155	348	-3.84
D	No data					
4 Jan., 1992						
I	472	3001	3094	159	886	-14.34
O	464	2724	2780	163	698	-11.06
D	424	2114	2394	177	475	-8.06
16 Jan., 1992						
I	478	3201	2921	142	737	-11.03
O	464	2875	2817	144	768	-13.14
D	431	2189	2245	159	654	-12.82
20 Jan., 1992						
I	493	3218	3256	157	929	-13.72
O	455	2733	2677	144	1105	-25.45
D	417	2096	2179	162	702	-17.80
13 Feb., 1992						
I	487	3372	3181	146	383	4.76
O	462	2930	2852	139	796	-13.86
D	427	2054	2104	159	693	-15.25
17 Feb., 1992						
I	507	3750	3773	156	180	-1.48
O	468	2833	2815	152	308	-3.42
D	416	1909	1996	157	509	-9.82
20 Mar., 1992						
I	505	3654	3856	164	163	-1.40
O	451	2629	2627	154	146	-1.41
D	No data					

FIGURE CAPTIONS

Fig. 1. Evolution of O_3 inside vortex (43). (A) Vertical distribution of O_3 mixing ratio inside vortex over period of mission. (B) Change in O_3 mixing ratio with respect to N_2O (14) using the O_3^{OCT} reference. Flights used and vortex boundaries are listed in Table 1. The three October flights are considered as a unit to represent the October O_3 and N_2O data. Data from the other flights in Table 1 are entered into the analyses individually.

Fig. 2. Plots of O_3 against N_2O during AASE II mission. (A) The three October flights to the pole (small closed circles) are compared with the February data inside the vortex (larger open circles). The heavy line is the O_3^{OCT} reference. (B) The outlines of the full range in monthly $O_3 - N_2O$ observations inside the vortex are overlaid in monthly sequence, with data below 420 K indicated for the months of January and February. The O_3^{OCT} reference is also shown. (C) The outline of Fig. 2B data is divided into the parcel types I, O, and D defined in text. Average Θ 's from 415 K to 510 K for October aircraft data are indicated as vertical bars. The extension of the October $O_3 - N_2O$ data to 50 ppbv $< N_2O < 130$ ppbv is from O_3 sonde and extrapolated aircraft data (29). (D) Aircraft data from inside and outside the vortex boundary during January and February, 1992 are plotted for $\Theta > 500$ K (squares and + 's) and $\Theta < 420$ K (circles and + 's).

Fig. 3. (A) Calculated daily O_3 loss rates (Table 2). (B) $O_3@155$ (Table 2) from 4 January through 17 February, with linear fits to the data from parcel types I, O, and D. Slopes of lines represent measured daily O_3 loss rates. (C) O_3 mass deficit (see text) in the air released from the bottom of the vortex.

Fig. 4. Cross section through vortex boundary of % O_3 change referenced through (A) O_3^{OCT} and (B) O_3^{EXT} . Data with $N_2O > 130$ ppbv from the four flights of 16 January through 17 February are taken as a unit then averaged to produce the contour (43). The horizontal coordinate was averaged over 1° of latitude.

REFERENCES AND NOTES

1. J.G. Anderson et al., *J. Geophys.Res.*, 94, 11480 (1989); J. Austin et al., *J. Geophys.Res.*, 94, 16717 (1989); J. G. Anderson, W. H. Brune, and M. H. Proffitt, *J. Geophys.Res.*, 94, 11465 (1989).
2. M. H. Proffitt et al., *J. Geophys.Res.*, 94, 16797 (1989).
3. J. W. Waters et al., *Nature*, 362,597 (1993).
4. M.H. Proffitt et al., *Nature*, 347,31 (1990).
5. Rumen D. Bojkov, *Meteorol. Atmos. Phys.*, 38, 117 (1988).
6. R. Stolarski et al., *Science*, 256,342 (1992).
7. WMO/UNEP Global Ozone Research and Monitoring Project Report No. 25, Executive summary (World Meteorological Organization, Geneva, 1991).
8. J. M. Rodriguez, M. K. W. Ko, N. D. Sze, *Nature*, 352,134 (1991); D. W. Fahey et al., AASE 11 paper submitted to *Nature*; D. J. Hofmann and S. Solomon, *J. Geophys.Res.*, 94,5029 (1989).
9. R J. Atkinson. et al., *Nature*, 340, 290 (1989); S. J. Reid and G. Vaughan, *Q.J.R. Meteorol. Soc.*, 117,825 (1991).
10. A. F. Tuck et al., *J. Geophys.Res.*, 97,7883 (1992).
11. Instruments are described in: M. H. Proffitt et al., *J. Geophys.Res.*, 94, 16547 (1989); W. H. Brune, J. G. Anderson, and K. R. Chan, *J. Geophys.Res.*, 94, 16649 (1989); K. R. Chan et al., *J. Geophys.Res.*, 94, 11573 (1989); M. Loewenstein, *J. Geophys.Res.*, 94, 11589 (1989); J. W. Elkins et al., *J. Geophys.Res.*, in preparation (1993).
12. The vortex interior has two different aspects: an outer ring generally within or near the polar night jet and characterized by high wind speeds and intermittent sunlight, and an inner vortex usually at the highest latitudes (nearer the pole) with much lower wind speeds and much less sunlight. Most of the flights during AASE 11 did not penetrate the inner vortex, therefore the data are considered as representative of the outer vortex.
13. L. M. Perliski, S. Solomon, and J. London, *J. Planet Space Sci.*, 37, 1527 (1989).
14. N_2O data were not available for 20 March so another conserved tracer CFC-11 was used in its place.
15. M. H. Proffitt et al., *Nature*, 342,233 (1989).
16. M. H. Proffitt, S. Solomon, and M. Loewenstein, *J. Geophys.Res.*, 97, 939 (1992).
17. O_3 loss occurs naturally during the summer at high latitudes (see J. C. Farman et al., *Quart. J. R. Met. Soc.* 111, 1013 (1985)) and must be considered when evaluating wintertime loss. If this O_3 poor air becomes trapped at high latitudes during vortex formation in early November and remain as an isolated pool through January and February, the reference function must represent the fall O_3 - N_2O relation.
18. M. H. Proffitt et al., *J. Geophys.Res.*, 94,11437 (1989).
19. M. R Schoeberl et al., *Geophys. Res. Lett.*, 17,469 (1990).
20. L.R. Lait et al., *Geophys. Res. Lett.*, 17,521 (1990).
21. A. F. Tuck, *J. Geophys. Res.*, 94,11,687 (1989).

22. C. R. Webster et al., Science, this issue (1993).
23. D. W. Toohey et al., Science, this issue (1993).
24. $\Theta = T(K) (1000/P(\text{mbar}))^{0.286}$.
25. E. V. Browell et al., Science, this issue (1993).
26. The fit was obtained from 6,8,12 October, 1991 ten second data. The O_3 and N_2O measurements were averaged into 8 equal Θ ranges from 360 to 520 K and a quadratic fit to these averages was calculated, thus weighting the data equally by Θ . An unweighed fit was compared and found to be almost identical except at the highest values of N_2O , where the O_3 was about 10% higher in the unweighed fit.
27. Air with $\text{N}_2\text{O} < 130$ ppbv was not accessible to the ER-2 early in the mission, but diabatic cooling brought much lower values within aircraft altitudes during January and February. Accordingly, parcels with $\text{N}_2\text{O} < 130$ ppbv are excluded from all comparisons with the October reference.
28. D. S. McKenna et al., Geophys.Res.Lett., 17,553 (1990).
29. Monthly averages of O_3 sonde data for October 1991 are calculated at five Θ levels from 530 K to 610 K for each of the two high latitude stations, Resolute (75° N) and Alert (82° N), thus providing some station to station variability. N_2O is estimated for the same five Θ levels by extrapolating a quadratic fit to the October N_2O -0 aircraft data. Θ has been limited to 610 K, since the extrapolation implies that the average N_2O mixing ratio at 610 K is 50 ppbv, therefore is an extreme limit for finding air with $\text{N}_2\text{O} > 130$ ppbv.
30. This exterior reference is calculated from 10 second data that are more than 2° of latitude outside the boundary of the vortex and with $\Theta > 420$ K. Data within 2° were excluded to avoid contamination of the exterior data with vortex data that fall outside our conservative choice for a vortex boundary, and $\Theta > 420$ K to exclude air parcels coming out of the bottom of the vortex. Equation 2 is practically identical to the fit to the 1989 AASE exterior data.
31. On only one occasion did we find air parcels with $\text{N}_2\text{O} < 140$ ppbv outside the vortex boundary, that being $< 1^\circ$ outside on 17 February. These parcels had the character of vortex air.
32. This is primarily due to the loss rate being nearly proportional to the square of the air density, therefore producing an enhanced loss at the higher pressures in type D and O parcels. (see D. M. Murphy, J.Geophys.Res., 96,5045 (1991)).
33. M. N. Jukes and M. E. McIntyre, Nature, 32.8, 590 (1987); D. L. Hartmann et al., J. Geophys.Res., 94,16779 (1989); M. R. Schoeberl and D. L.Hartmann, Science, 251,46 (1991).
34. E. F. Danielsen and H. Houben, Anthropogene Beeinflussung der Ozonschicht, DECHEMA - Frankfurt am Main, ISBN 3-926959-0445, 191 (1988).
35. M. R. Schoeberl et al., J.Geophys.Res., 97,7859 (1992).
36. Alan Plumb, Nature (News and Views), 347,20 (1990).

37. R. J. Salawitch et al., *Science*, this issue (1993).
38. M. Patrick McCormick, Robert E. Veiga, and William P. Chu, *Geophys. Res. Lett.*, 19, 269 (1992). They report statistically significant (2σ) decreases below 18 km and 19 km respectively, and show negative trends increasing down to 15 km.
39. The rate of descent at the bottom of the vortex (w) can be estimated, by assuming diabatic cooling rates of 1 K/day, multiplied times the measured vertical gradients in Θ . Since most of the data are in the outer ring, the area of descent (A) has been limited to $1.2 \times 10^{13} \text{m}^2$, an area equivalent to that from 65°N to 72°N , or approximately half the area of the vortex. $\text{N}_2\text{O} > 150$ ppbv at the bottom of the vortex so within the range for the functions O_3^{OCT} and O_3^{EXT} . Our calculations result in a conservative estimate of total O_3 mass destroyed.
40. A flight on 6 January, 1992 also penetrated the polar vortex but data were not available from all of the instruments.
41. D. W. Toohey et al., *Geophys. Res. Lett.*, 17, 513 (1990).
42. Jet Propulsion Laboratory, Publ. 92-20, Pasadena, CA (1990).
43. Contour plots are produced using DeltaGraph® Professional v. 2.0.2 software to produce XYZ contour line plots. The contoured data are averaged into 7 equal theta ranges from 380 K to 560 K. All data are plotted without smoothing and usually appear as sharp corners. The data are equally weighted with linear interpolations on triangular grids between data points to span the gaps.
44. We thank J.G. Anderson, D. W. Toohey, L. M. Avallone, L. R. Lait, P. A. Newman, M. R. Schoeberl, E. Danielsen, D. W. Fahey, and A. F. Tuck, for their contributions.

ACKNOWLEDGMENT

A portion of this research was carried out by the Jet Repulsion Laboratory, California Institute of Technology, under a contract with the National Aeronautics and Space Administration.

FIGURE 1A
INSIDE VORTEX

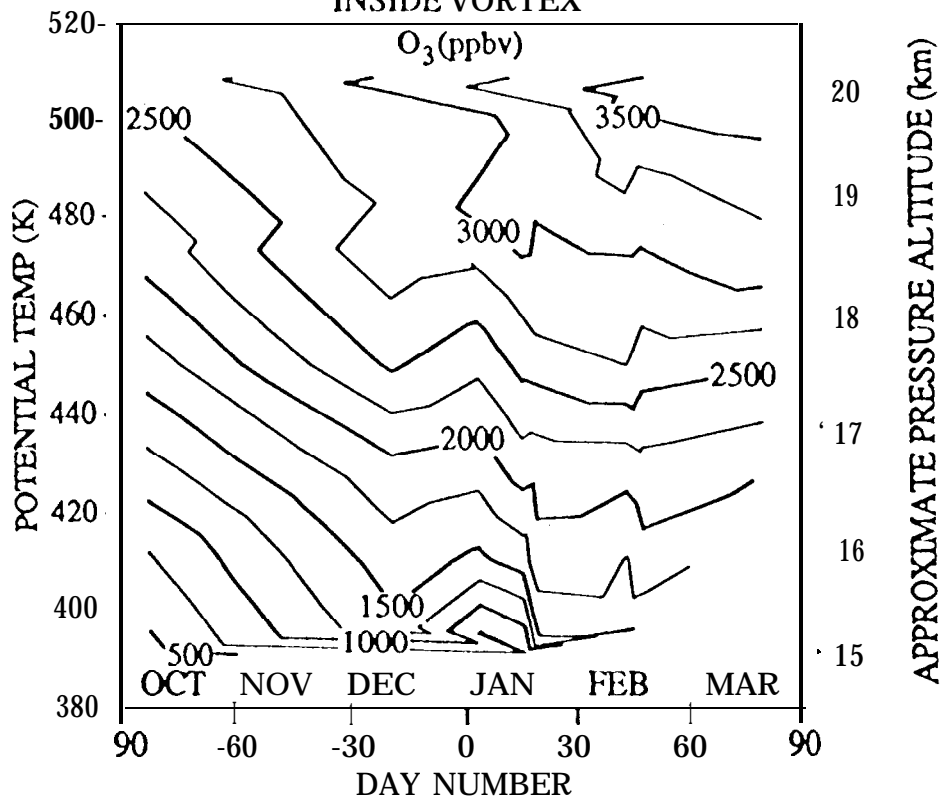


FIGURE 1B
INSIDE VORTEX

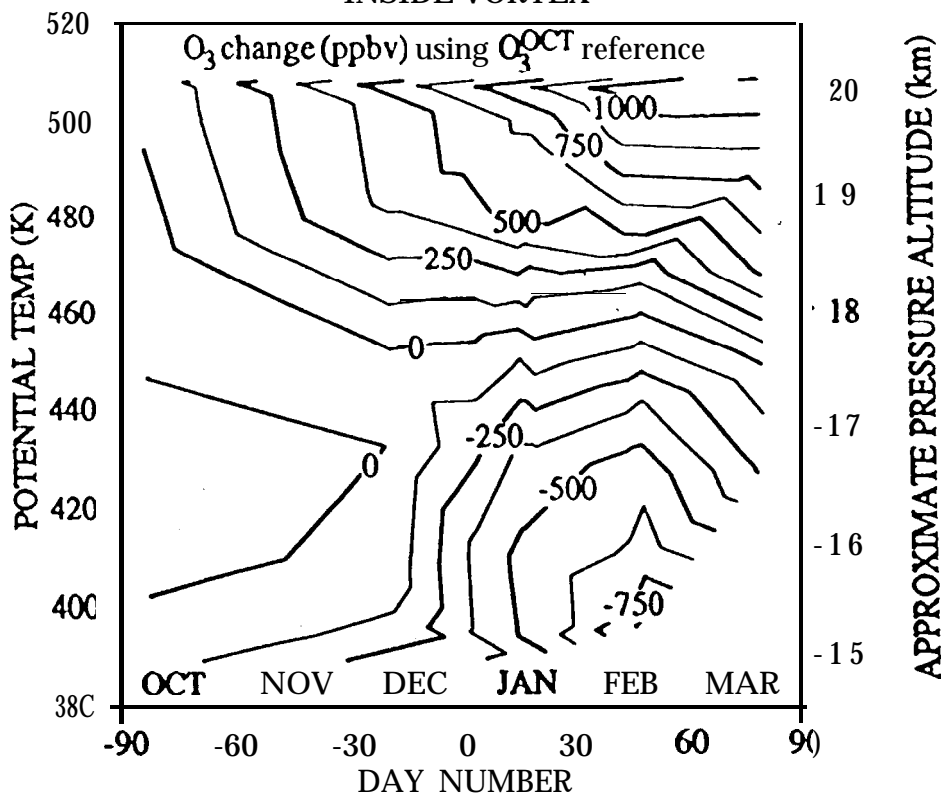


FIGURE 2A

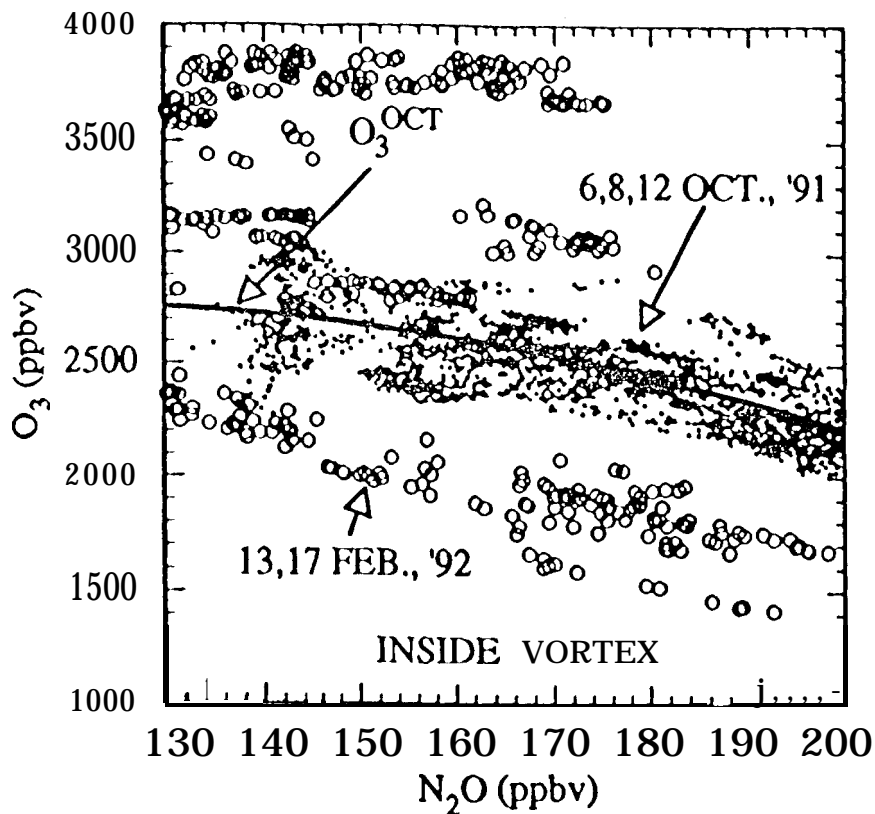


FIGURE 2B

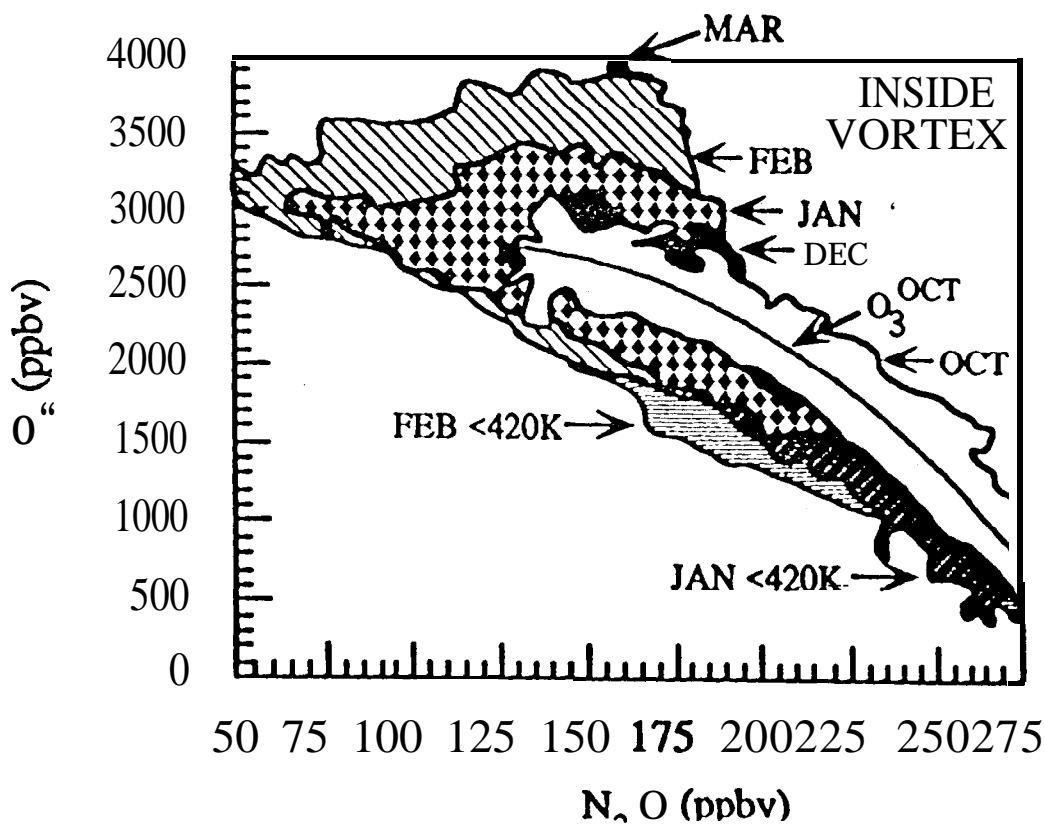


FIGURE 2C

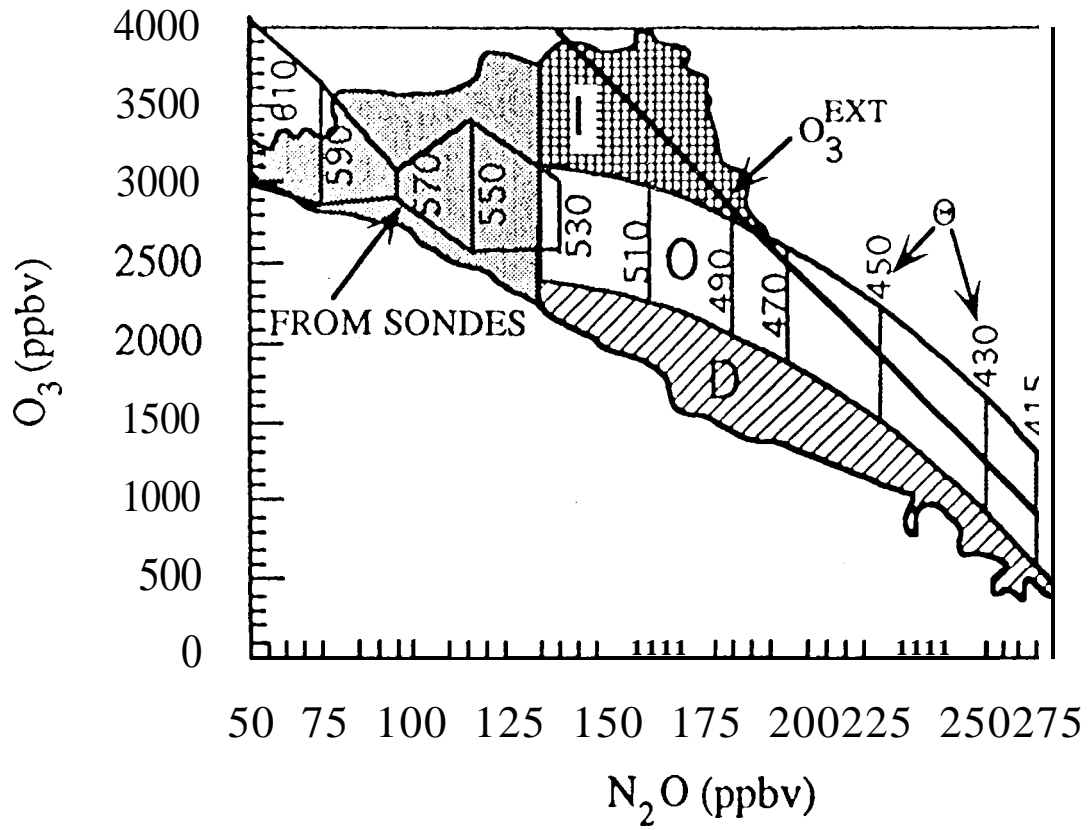


FIGURE 2D

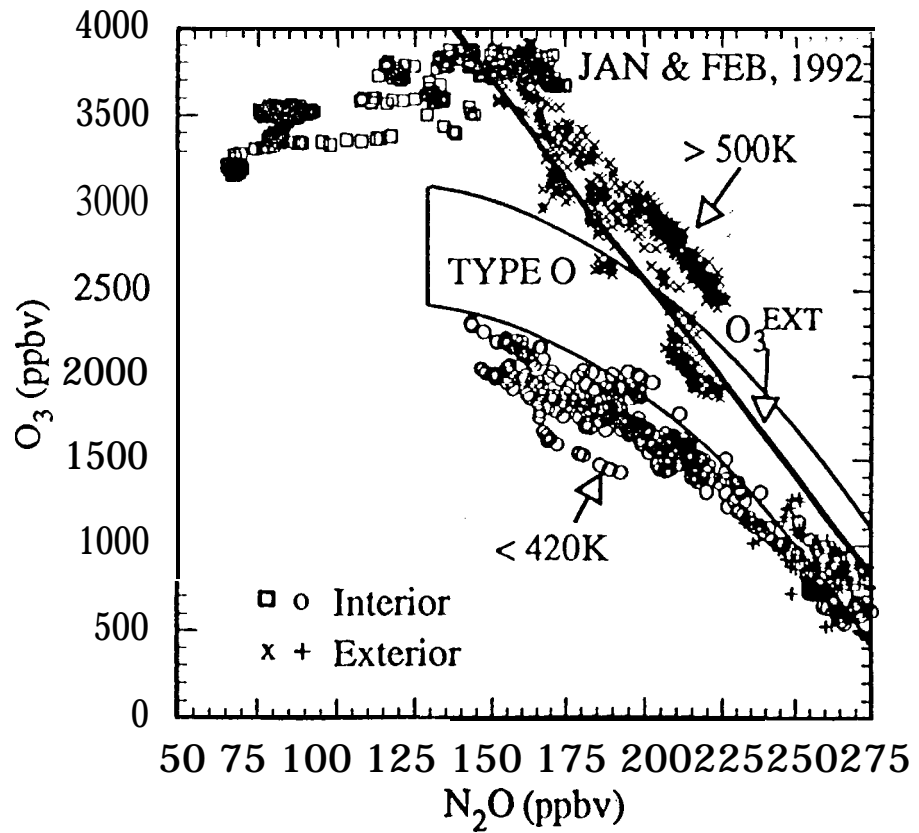


FIGURE 3A

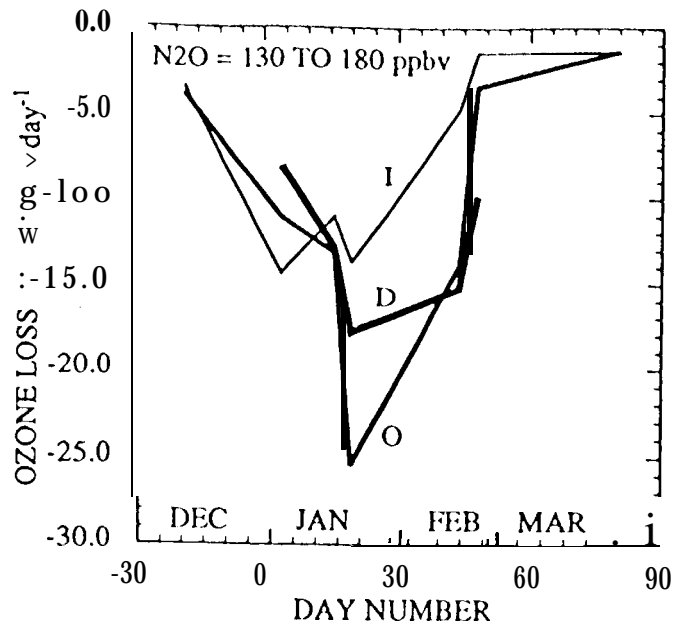


FIGURE 3B

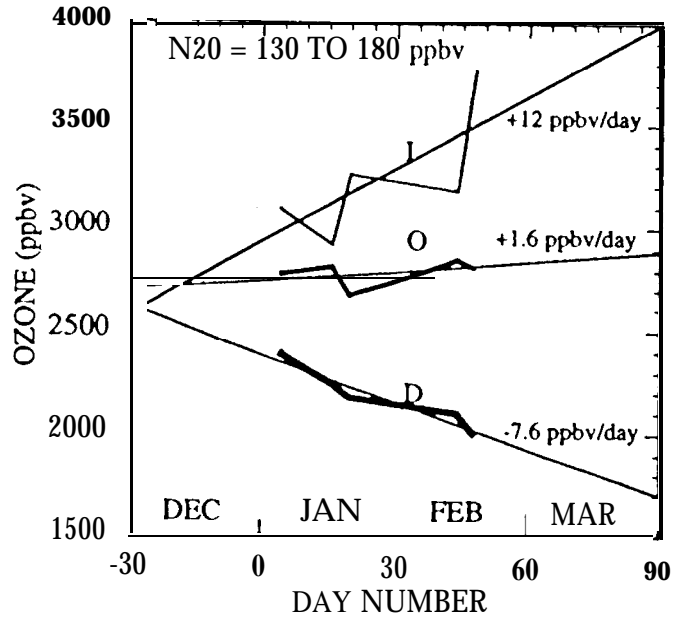


FIGURE 3C

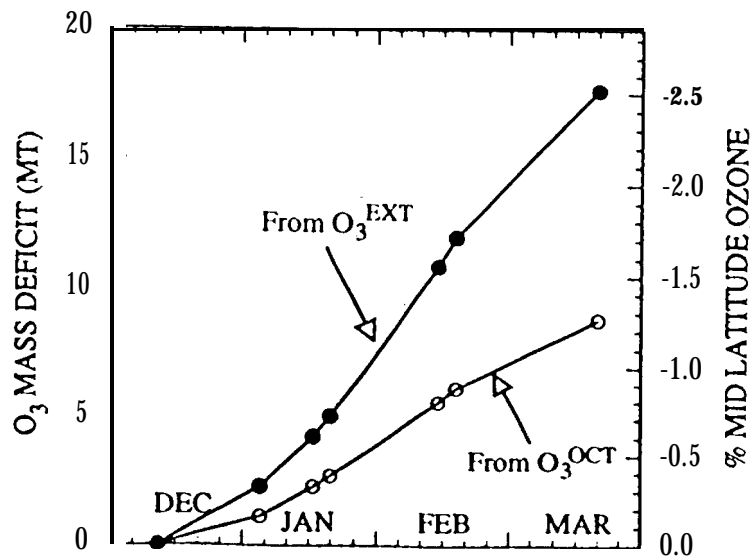


FIGURE 4A

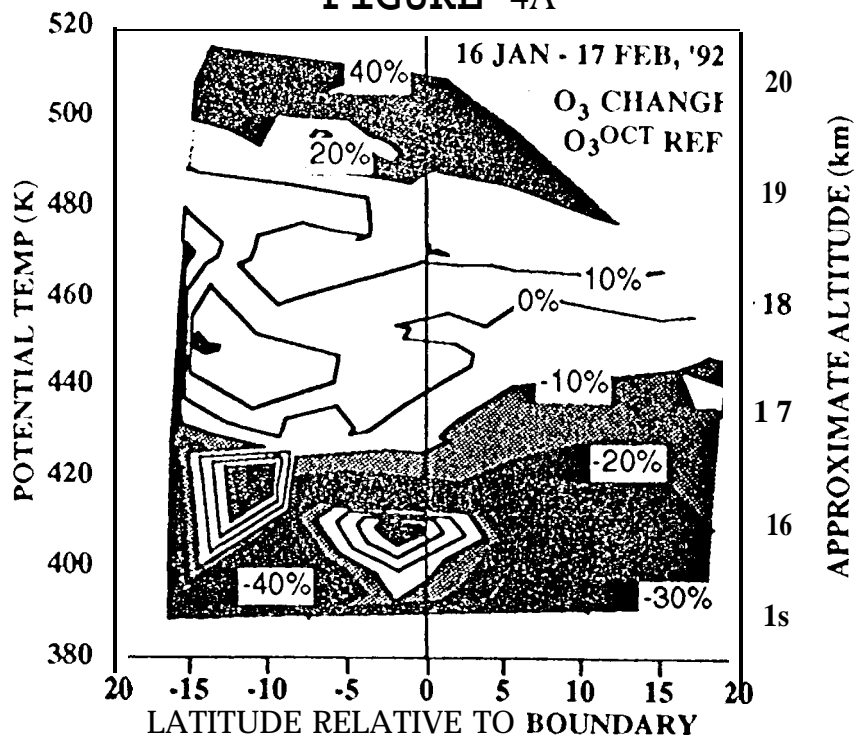


FIGURE 4B

